Frequency-dependent conductivity in polycrystalline metals and semiconductors

Bruce J. Palmer and Roy Gordon
Department of Chemistry, Harvard University, Cambridge, Massachusetts 02138
(Received 17 April 1989; revised manuscript received 28 August 1989)

We develop a simple theory of conductivity in polycrystalline metals and heavily doped semiconductors. We start with the ordinary Drude theory of conductivity and extend it to include a spatially dependent scattering frequency. We also explicitly include the local electric fields created by fluctuations in the electron density. The crystal grains are described as low-scattering regions surrounded by thin walls of highly scattering material. This model can be expressed as a linear Boltzmann equation and can be solved exactly with use of an appropriate orthonormal basis. We find that the presence of grain boundaries can alter the qualitative behavior of the conductivity.

I. INTRODUCTION

Although many solids are commonly used in polycrystalline form, relatively little is known theoretically about how polycrystallinity affects material properties and many questions about transport and structure remain to be explored. In this paper we will focus on transport and attempt to develop a microscopic theory of the frequency-dependent conductivity in polycrystalline metals and heavily doped semiconductors.

Our interest was originally motivated by the observation that reflectance spectra from polycrystalline thin films often deviate significantly from a typical Drude-like curve.[1–4] Since the reflectance spectrum is a probe of the frequency-dependent conductivity, it is natural to ask what effect the grain boundaries have on transport. To answer this we started with a Boltzmann equation for the conduction electrons. Although the Boltzmann equation is essentially a classical approach, quantum-mechanical properties of the electrons can be incorporated by using the semiclassical equations of motion for electrons in a metal or *n*-type doped semiconductor. These equations can be used to construct the drift operator describing the evolution of the one-particle distribution function for electrons in the absence of collisions.

Electron-electron scattering is relatively unimportant compared to scattering by lattice defects, impurities, and phonons in metals and heavily doped semiconductors. These effects can usually be included in a Boltzmann equation via a linear collision operator and all the extensive machinery for solving linear equations can be brought to bear on the problem. Both variational techniques[5–7] and diagonalization on an appropriate orthonormal basis[8–10] have been used to calculate transport coefficients. In all these calculations it has been assumed that the sample is statistically isotropic with respect to translations (nonspherical Fermi surfaces will destroy rotational invariance). This represents an important simplification since the one-particle distribution function must therefore be independent of position and the amount of computation required to compute transport coefficients is considerably reduced.

For grain-boundary scattering it is no longer clear whether or not it is possible to ignore the spatial distribution of scatterers. In this case the grain boundaries represent highly localized planar regions characterized by high scattering probabilities surrounding crystal grains with relatively low scattering probabilities. Previous attempts to model the effect of grain boundaries have involved calculating a scattering operator that has been averaged over the grain-boundary locations and using this to compute the conductivity.[11–15] Considering the averaged grain-boundary scattering again eliminates the spatial degrees of freedom but it is difficult to assess how this affects the final answer. In particular, can a spatially uniform process be used to approximate inhomogeneous scattering?

In systems where the grains are large we expect a negligible contribution to the transport properties. However, in many cases the grains are small, the surface-to-volume ratio is large, and the effects due to grain boundaries must be taken into account. This situation can occur in the case of heavily doped semiconductors.

Our approach is to consider a fairly simple system in which we include spatial variation explicitly. We start with the Drude theory of electrons in a metal or semiconductor and write this in the form of a linear Boltzmann equation. The grain boundaries are modeled as spatial nonuniformities in the scattering frequency. The Boltzmann equation is converted to a matrix integral equation using standard techniques and inverted. We find that under certain conditions the inclusion of grain-boundary scattering can alter the qualitative behavior of the conductivity.

II. DRUDE MODEL WITH SPATIALLY INHOMOGENEOUS SCATTERING

A semiclassical theory for the transport of electrons in a metal with grain boundaries can be written down by allowing the scattering term in the usual Boltzmann equation to have a spatial dependence. The grain boundaries can then be depicted as localized regions of high scattering. Following Ziman,[16] we start with the equation

$$\frac{\partial f_{\mathbf{k}}}{\partial t}+\mathbf{v}\cdot\nabla_{\mathbf{r}}f_k-\frac{e}{\hbar}\mathbf{E}_{\rm tot}\cdot\nabla_{\mathbf{k}}f_{\mathbf{k}} =\int d^3k'[f_{\mathbf{k}'}(1-f_{\mathbf{k}})-f_{\mathbf{k}}(1-f_{\mathbf{k}'})]\mathcal{Q}(\mathbf{k},\mathbf{k}',\mathbf{r}) , \tag{2.1}$$

where the $f_{\mathbf{k}}$ are the semiclassical approximations to the one-particle quantum-mechanical distribution functions for fermions. The spatial dependence is located in the scattering amplitudes $\mathcal{Q}(\mathbf{k},\mathbf{k}',\mathbf{r})$. The factors of $(1-f_{\mathbf{k}})$ ensure that the final state for the scattering event is empty, as required by the Pauli principle. However, because of microscopic reversibility, $\mathcal{Q}(\mathbf{k},\mathbf{k}',\mathbf{r})=\mathcal{Q}(\mathbf{k}',\mathbf{k},\mathbf{r})$ and the terms quadratic in $f_{\mathbf{k}}$ cancel, leaving

$$\frac{\partial f_{\mathbf{k}}}{\partial t}+\mathbf{v}\cdot\nabla_{\mathbf{r}}f_{\mathbf{k}}-\frac{e}{\hbar}\mathbf{E}_{\rm tot}\cdot\nabla_{\mathbf{k}}f_{\mathbf{k}} =-f_{\mathbf{k}}\int d^3k'\,\mathcal{Q}(\mathbf{k},\mathbf{k}',\mathbf{r})+\int d^3k'\,\mathcal{Q}(\mathbf{k},\mathbf{k}',\mathbf{r})f_{\mathbf{k}'} . \tag{2.2}$$

Making a relaxation-time approximation on the scattering terms then gives the equation

$$\frac{\partial f_{\mathbf{k}}}{\partial t}+\mathbf{v}\cdot\nabla_{\mathbf{r}}f_{\mathbf{k}}-\frac{e}{\hbar}\mathbf{E}_{\rm tot}\cdot\nabla_{\mathbf{k}}f_{\mathbf{k}}=-\gamma(\mathbf{r})f_{\mathbf{k}}+\gamma(\mathbf{r})f_{\rm LE} , \tag{2.3}$$

where $f_{\rm LE}$ is the local-equilibrium distribution function and $\gamma(\mathbf{r})$ is a spatially dependent scattering frequency.

In our equations we prefer to use electron velocities instead of momenta. This can be done using the semiclassical equations of motion[16,17]

$$\mathbf{v}(\mathbf{k})=\frac{1}{\hbar}\frac{\partial\varepsilon(\mathbf{k})}{\partial\mathbf{k}} , \tag{2.4}$$

$$\hbar\dot{\mathbf{k}}=-e\mathbf{E} , \tag{2.5}$$

where $\varepsilon(\mathbf{k})$ is the energy of an electron in the conduction band with wave vector $\mathbf{k}$ and $\mathbf{E}$ is the local electric field. Assuming that the energy-dispersion relation is approximately that of a free-electron gas, we can then make the substitution

$$\frac{1}{\hbar}\nabla_{\mathbf{k}}\rightarrow\frac{1}{m}\nabla_{\mathbf{v}}$$

and Eq. (2.3) becomes

$$\frac{\partial f}{\partial t}+\mathbf{v}\cdot\nabla_{\mathbf{r}}f-\frac{e}{m}\mathbf{E}_{\rm tot}(t)\cdot\nabla_{\mathbf{v}}f=-\gamma(\mathbf{r})f+\gamma(\mathbf{r})f_{\rm LE} . \tag{2.6}$$

Equation (2.6) is the Boltzmann equation for a Drude electron in a system with a spatially dependent scattering frequency. It has the following simple physical interpretation.[17]

(i) Between collisions electrons act as free particles.

(ii) Collisions are instantaneous. Because of this the local density remains unchanged.

(iii) Electrons are completely "thermalized" by a collision, i.e., the probability of an electron having velocity $\mathbf{v}$ after a collision is determined by the local-equilibrium velocity distribution $f_{\rm LE}$.

(iv) Electrons undergo collisions with a frequency γ so the probability of a collision occurring in a time interval dt is $\gamma\,dt$.

In the traditional Drude model γ is constant throughout the system. The assumptions (i)-(iv) can then be reduced to a set of simple first-order equations that are readily solved. However, inclusion of the space dependence complicates the mathematical analysis considerably.

The Fermi temperature is assumed to be sufficiently high that we can choose $f_{\rm LE}$ to have the zero-temperature form

$$f_{\rm LE}=\frac{n_0}{V_F}\Theta(\epsilon_F+\delta\mu-\tfrac{1}{2}m\mathbf{v}^2) , \tag{2.7}$$

where $\Theta(x)$ is the Heaviside step function, V_F is the volume of the Fermi sphere in velocity space, $V_F=4\pi v_F^3/3$, v_F is the Fermi velocity, and n_0 is the equilibrium density of electrons. $\delta\mu$ is the local variation in the chemical potential. In the absence of the external field, $\delta\mu=0$. The constants out in front of the step function ensure that f has the normalization

$$n(\mathbf{r},t)=\int d^3v\,f_{\rm LE} .$$

$\delta\mu$ is determined by the requirement that $f_{\rm LE}$ integrates down to the correct density. Expanding $f_{\rm LE}$ to first order in $\delta\mu$ gives

$$f_{\rm LE}=\frac{n_0}{V_F}\Theta(\epsilon_F-\tfrac{1}{2}m\mathbf{v}^2)+\frac{n_0}{V_F}\delta(\epsilon_F-\tfrac{1}{2}m\mathbf{v}^2)\delta\mu(\mathbf{r},t) =\frac{n_0}{V_F}\Theta(\epsilon_F-\tfrac{1}{2}m\mathbf{v}^2)+\frac{n_0}{V_F}\frac{1}{mv_F}\delta(v_F-v)\delta\mu(\mathbf{r},t) . \tag{2.8}$$

We have used some well-known properties of δ functions to write the second line. Integrating both sides of Eq. (2.8) over $\mathbf{v}$ gives us our relation between $\delta\mu(\mathbf{r},t)$ and $\delta n(\mathbf{r},t)$,

$$n(\mathbf{r},t)=n_0+n_0\frac{3}{mv_F^2}\delta\mu(\mathbf{r},t) ,$$

which is easily solved for $\delta\mu(\mathbf{r},t)$,

$$\delta\mu(\mathbf{r},t)=\frac{mv_F^2}{3n_0}\delta n(\mathbf{r},t) .$$

$f_{\rm LE}$ can now be written as

$$f_{\rm LE}=\frac{n_0}{V_F}\Theta(v_F-v)+\frac{n_0}{4\pi v_F^2}\delta(v_F-v)\delta n(\mathbf{r},t) . \tag{2.9}$$

In the absence of any spatial variation in the system $\mathbf{E}_{\rm tot}$ is the applied external field. Translational invariance guarantees that the density of electrons is uniform and prevents the creation of local electric fields. If we break translational symmetry by introducing spatially depen-

dent scattering, the resulting density fluctuations will lead to the creation of local fields, which we denote by $\mathbf{E}_{\rm loc}$. $\mathbf{E}_{\rm tot}$ is then of the form

$$\mathbf{E}_{\rm tot}=\mathbf{E}_{\rm ext}+\mathbf{E}_{\rm loc} ,$$

where $\mathbf{E}_{\rm loc}$ is

$$\mathbf{E}_{\rm loc}=-\frac{e}{\epsilon_0}\int d^3r'\frac{\mathbf{r}-\mathbf{r}'}{|\mathbf{r}-\mathbf{r}'|^3}[n(\mathbf{r}',t)-n_0] .$$

n_0 is the equilibrium density of electrons and ϵ_0 is the static dielectric constant for the atomic cores. Using these expressions in (2.6) we arrive at the equation

$$\frac{\partial f}{\partial t}+\mathbf{v}\cdot\nabla_{\rm r}f-\frac{e}{m}\left[\mathbf{E}_{\rm ext}-\frac{e}{\epsilon_0}\int d^3r'\frac{\mathbf{r}-\mathbf{r}'}{|\mathbf{r}-\mathbf{r}'|^3}[n(\mathbf{r}',t)-n_0]\right]\cdot\nabla_{\rm v}f=-\gamma(\mathbf{r})f+\gamma(\mathbf{r})f_{\rm LE} . \tag{2.10}$$

Since $n(\mathbf{r},t)$ is proportional to f the local fields add a quadratic term to the Boltzmann equation. In addition, $f_{\rm LE}$ is generally a nonlinear functional of the density. However, we can still linearize this about the external field to get a linear equation. To do this we begin by noting that the zero-field solution of Eq. (2.10) is

$$f_0=n_0\frac{1}{V_F}\Theta(v_F-v) . \tag{2.11}$$

This can be verified by direct substitution and noting that for zero field $\delta n=0$. For simplicity we assume that the external field is located along the z axis. The full distribution function f can then be expanded as a power series in E_z about the zero-field solution, f_0,

$$f=f_0+gE_z+O(E_z^2) . \tag{2.12}$$

We are only interested in the response of the system to order E_z so we ignore terms of order E_z^2 and higher. Inserting (2.9) and (2.12) into (2.10) and retaining terms to order E_z gives

$$\frac{\partial g}{\partial t}E_z+g\frac{\partial E_z}{\partial t}+\mathbf{v}\cdot\nabla_{\rm r}(gE_z)+\frac{e^2}{\epsilon_0 m}\left[\int d^3r'\frac{\mathbf{r}-\mathbf{r}'}{|\mathbf{r}-\mathbf{r}'|^3}\int d^3v'g\right]\cdot\nabla_{\rm v}f_0E_z$$
$$+\gamma(\mathbf{r})gE_z-\gamma(\mathbf{r})\frac{1}{4\pi v_F^2}\delta(v_F-v)\int d^3v'gE_z=\frac{e}{m}\frac{\partial f_0}{\partial v_z}E_z . \tag{2.13}$$

Since g represents the linear corrections to f due to the external field we can choose $E_z(t)$ to have the form

$$E_z(t)=E_z e^{i\omega t} .$$

Using this in Eq. (2.13) gives the following equation for g:

$$\frac{\partial g}{\partial t}+i\omega g+\mathbf{v}\cdot\nabla_{\rm r}g+\frac{e^2}{\epsilon_0 m}\left[\int d^3r'\frac{\mathbf{r}-\mathbf{r}'}{|\mathbf{r}-\mathbf{r}'|^3}\int d^3v'g\right]\cdot\nabla_{\rm v}f_0+\gamma(\mathbf{r})g-\gamma(\mathbf{r})\frac{1}{4\pi v_F^2}\delta(v_F-v)\int d^3v'g=\frac{e}{m}\frac{\partial f_0}{\partial v_z} . \tag{2.14}$$

Equation (2.14) is an inhomogeneous linear equation. Since the inhomogeneous term is time independent, this suggests that g is also time independent and we can set the time derivative of g in (2.14) equal to zero to get

$$i\omega g+\mathbf{v}\cdot\nabla_{\rm r}g+\frac{e^2}{\epsilon_0 m}\left[\int d^3r'\frac{\mathbf{r}-\mathbf{r}'}{|\mathbf{r}-\mathbf{r}'|^3}\int d^3v'g\right]\cdot\nabla_{\rm v}f_0+\gamma(\mathbf{r})g-\gamma(\mathbf{r})\frac{1}{4\pi v_F^2}\delta(v_F-v)\int d^3v'g=\frac{e}{m}\frac{\partial f_0}{\partial v_z} . \tag{2.15}$$

This is the equation on which we will base the remainder of our analysis.

III. MATRIX METHOD OF SOLUTION

In this section we convert Eq. (2.15) into a matrix integral equation. We begin by making our system periodic on all three axes with period L. The scattering function $\gamma(\mathbf{r})$ can then be expanded as

$$\gamma(\mathbf{r})=\sum_{\mathbf{k}}\gamma(\mathbf{k})e^{i\mathbf{k}\cdot\mathbf{r}} . \tag{3.1}$$

The wave vectors $\mathbf{k}$ are of the form

$$\mathbf{k}=\left[n_1\frac{2\pi}{L}, n_2\frac{2\pi}{L}, n_3\frac{2\pi}{L}\right],$$

where n_1, n_2, and n_3 are integers. The spatial dependence of g must also be periodic so g can be written as

$$g=\sum_{\mathbf{k}} g(\mathbf{k},\mathbf{v})e^{i\mathbf{k}\cdot\mathbf{r}} . \tag{3.2}$$

We can further expand (3.2) by expressing the angular part of $\mathbf{v}$ in terms of the spherical harmonics $Y_{lm}(\theta,\phi)$. In this paper the variables θ and ϕ will always refer to the angular part of the velocity vector $\mathbf{v}$. Equation (3.2) becomes

$$g=\sum_{\mathbf{k}}\sum_{l,m} g_{lm}(\mathbf{k},v)Y_{lm}(\theta,\phi)e^{i\mathbf{k}\cdot\mathbf{r}} . \tag{3.3}$$

The next step is to substitute these expansions into Eq. (2.15). However, because the term due to the local fields is so much more complicated than the rest of the equation, we temporarily assume that it is zero. We treat it separately in the next section. Substituting the expansions (3.1) and (3.3) into the remaining terms in (2.15) gives

$$\sum_{l,m} i\omega g_{lm}(\mathbf{k},v)Y_{lm}(\theta,\phi)+\sum_{l,m} i\mathbf{k}\cdot\mathbf{v}g_{lm}(\mathbf{k},v)Y_{lm}(\theta,\phi)+\sum_{\mathbf{k}'}\sum_{l',m'}\gamma(\mathbf{k}-\mathbf{k}')g_{l'm'}(\mathbf{k}',v)Y_{l'm'}(\theta,\phi)$$
$$-\sum_{\mathbf{k}'}\frac{1}{v_F^2}\delta(v_F-v)\gamma(\mathbf{k}-\mathbf{k}')\int dv'(v')^2 g_{00}(\mathbf{k}',v')Y_{00}(\theta,\phi)=\frac{e}{m}\frac{\partial f_0}{\partial v_z} . \tag{3.4}$$

In arriving at (3.4) we have equated all the coefficients of $\exp(i\mathbf{k}\cdot\mathbf{r})$. Only the $Y_{00}(\theta,\phi)$ term survives the angular integration. The second term in (3.4) has not been completely expanded in the spherical harmonics. The cartesian components of the vector $\mathbf{v}$ can be expressed as

$$v_x=-v\left[\frac{2\pi}{3}\right]^{1/2}[Y_{11}(\theta,\phi)-Y_{1,-1}(\theta,\phi)] ,$$
$$v_y=iv\left[\frac{2\pi}{3}\right]^{1/2}[Y_{11}(\theta,\phi)+Y_{1,-1}(\theta,\phi)] ,$$
$$v_z=v\left[\frac{4\pi}{3}\right]^{1/2}Y_{10}(\theta,\phi) .$$

The term $i\mathbf{k}\cdot\mathbf{v}$ can then be written as

$$i\mathbf{k}\cdot\mathbf{v}=\sum_{m=-1}^{m=1}\nu_m(\mathbf{k},v)Y_{1m}(\theta,\phi) , \tag{3.5}$$

where the coefficients $\nu_m(\mathbf{k},v)$ are given by

$$\nu_1(\mathbf{k},v)=-iv\left[\frac{2\pi}{3}\right]^{1/2}(k_x-ik_y) ,$$
$$\nu_0(\mathbf{k},v)=iv\left[\frac{4\pi}{3}\right]^{1/2}k_z , \tag{3.6}$$
$$\nu_{-1}(\mathbf{k},v)=iv\left[\frac{2\pi}{3}\right]^{1/2}(k_x+ik_y) .$$

For $m\neq -1,0,1$ we define the $\nu_m(\mathbf{k},v)$ to be identically zero. Using the expansion (3.5) in (3.4) we obtain

$$\sum_{\mathbf{k}'}\sum_{l,m}\sum_{l',m'} i\omega\delta_{\mathbf{k}\mathbf{k}'}\delta_{ll'}\delta_{mm'}g_{l'm'}(\mathbf{k}',v)Y_{l'm'}(\theta,\phi)+\sum_{\mathbf{k}'}\sum_{l',m'}\sum_{m=-1}^{m=1}\nu_m(\mathbf{k},v)\delta_{\mathbf{k}\mathbf{k}'}g_{l'm'}(\mathbf{k}',v)Y_{1m}(\theta,\phi)Y_{l'm'}(\theta,\phi)$$
$$+\sum_{\mathbf{k}'}\sum_{l',m'}\gamma(\mathbf{k}-\mathbf{k}')g_{l'm'}(\mathbf{k}',v)Y_{l'm'}(\theta,\phi)-\sum_{\mathbf{k}'}\sum_{l'm'}\frac{1}{v_F^2}\delta(v_F-v)\gamma(\mathbf{k}-\mathbf{k}')\delta_{l'0}\delta_{m'0}$$
$$\times\int dv'(v')^2 g_{l'm'}(\mathbf{k}',v')Y_{l'm'}(\theta,\phi)=-\frac{en_0}{m}\frac{1}{V_F}\delta(v_F-v)\frac{v_z}{v} . \tag{3.7}$$

The Kronecker delta symbols have been used to introduce a few extra summations.

The second term in (3.7) is quadratic in the $Y_{lm}(\theta,\phi)$'s. From the theory of addition of angular momentum we can decompose the product of spherical harmonics using the formula[18]

$$Y_{l_1m_1}(\theta,\phi)Y_{l_2m_2}(\theta,\phi)=\sum_L\left[\frac{(2l_1+1)(l_2+1)}{4\pi(2L+1)}\right]^{1/2}\langle l_1l_200|l_1l_2L0\rangle\langle l_1l_2m_1m_2|l_1l_2L,m_1+m_2\rangle Y_{L,m_1+m_2}(\theta,\phi) ,$$

where $\langle l_1l_2m_1m_2|l_1l_2L,m_1+m_2\rangle$ are Clebsch-Gordan coefficients. Equation (3.7) can then be written as

$$\sum_{\mathbf{k}'}\sum_{l,m}\sum_{l',m'} i\omega\delta_{\mathbf{k}\mathbf{k}'}\delta_{ll'}\delta_{mm'}g_{l'm'}(\mathbf{k}',v)Y_{l'm'}(\theta,\phi)+\sum_{\mathbf{k}'}\sum_{l,m}\sum_{l',m'}\left[\frac{3(2l'+1)}{4\pi(2l+1)}\right]^{1/2}\langle l'100|l'1l0\rangle\langle l'1m'm|l'1l,m+m'\rangle$$
$$\times\nu_m(\mathbf{k},v)\delta_{\mathbf{k}\mathbf{k}'}g_{l'm'}(\mathbf{k}',v)Y_{l,m+m'}(\theta,\phi)+\sum_{\mathbf{k}'}\sum_{l',m'}\gamma(\mathbf{k}-\mathbf{k}')g_{l'm'}(\mathbf{k}',v)Y_{l'm'}(\theta,\phi)$$
$$-\sum_{\mathbf{k}'}\sum_{l',m'}\frac{1}{v_F^2}\delta(v_F-v)\gamma(\mathbf{k}-\mathbf{k}')\delta_{l'0}\delta_{m'0}\int dv'(v')^2 g_{l'm'}(\mathbf{k}',v')Y_{l'm'}(\theta,\phi)$$
$$=\sum_{l,m}-\left[\frac{4\pi}{3}\right]^{1/2}\frac{en_0}{m}\frac{1}{V_F}\delta(v_F-v)\delta_{l1}\delta_{m0}Y_{lm}(\theta,\phi)\ . \tag{3.8}$$

Analytical expressions for the Clebsch-Gordan coefficients appearing in (3.8) have been tabulated.[19]

To identify the coefficients of the $Y_{lm}(\theta,\phi)$ in (3.8) we make the substitution $m'+m\rightarrow m'$ in the first term on the left-hand side of (3.8) and relabel the sums in the remaining terms as sums over (l,m) instead of (l',m'). Equation (3.8) becomes

$$\sum_{\mathbf{k}'}\sum_{l,m}\sum_{l',m'} i\omega\delta_{\mathbf{k}\mathbf{k}'}\delta_{ll'}\delta_{mm'}g_{lm}(\mathbf{k}',v)Y_{lm}(\theta,\phi)+\sum_{\mathbf{k}'}\sum_{l,m}\sum_{l',m'}\left[\frac{3(2l'+1)}{4\pi(2l+1)}\right]^{1/2}\langle l'100|l'1l0\rangle\langle l'1m',m-m'|l'1lm\rangle$$
$$\times\nu_{m-m'}(\mathbf{k},v)\delta_{\mathbf{k}\mathbf{k}'}g_{l'm'}(\mathbf{k}',v)Y_{lm}(\theta,\phi)+\sum_{\mathbf{k}'}\sum_{l,m}\gamma(\mathbf{k}-\mathbf{k}')g_{lm}(\mathbf{k}',v)Y_{lm}(\theta,\phi)$$
$$-\sum_{\mathbf{k}'}\sum_{l,m}\frac{1}{v_F^2}\delta(v_F-v)\gamma(\mathbf{k}-\mathbf{k}')\delta_{l0}\delta_{m0}\int dv'(v')^2 g_{lm}(\mathbf{k}',v')Y_{lm}(\theta,\phi)$$
$$=-\sum_{l,m}\left[\frac{4\pi}{3}\right]^{1/2}\frac{en_0}{m}\frac{1}{V_F}\delta(v_F-v)\delta_{l1}\delta_{m0}Y_{lm}(\theta,\phi)\ . \tag{3.9}$$

Equating the coefficients of the $Y_{lm}(\theta,\phi)$ yields

$$\sum_{\mathbf{k}'}\sum_{l',m'}\left[i\omega\delta_{\mathbf{k}\mathbf{k}'}\delta_{ll'}\delta_{mm'}g_{l'm'}(\mathbf{k}',v)+\left[\frac{3(2l'+1)}{4\pi(2l+1)}\right]^{1/2}\langle l'100|l'1l0\rangle\langle l'1m',m-m'|l'1lm\rangle\right.$$
$$\times\nu_{m-m'}(\mathbf{k},v)\delta_{\mathbf{k}\mathbf{k}'}g_{l'm'}(\mathbf{k}',v)+\gamma(\mathbf{k}-\mathbf{k}')\delta_{ll'}\delta_{mm'}g_{l'm'}(\mathbf{k}',v)$$
$$\left.-\frac{1}{v_F^2}\delta(v_F-v)\gamma(\mathbf{k}-\mathbf{k}')\delta_{ll'}\delta_{mm'}\delta_{l0}\delta_{m0}\int dv'(v')^2 g_{l'm'}(k',v')\right]=-\left[\frac{4\pi}{3}\right]^{1/2}\frac{en_0}{m}\frac{1}{V_F}\delta(v_F-v)\delta_{l1}\delta_{m0}\ . \tag{3.10}$$

We have extended the summation over (l',m') to all terms on the left-hand side of (3.10) by including a few extra Kronecker delta symbols. Equation (2.15) is now explicitly in the form of a matrix integral equation. We can write it as

$$\mathsf{A}(v)\cdot\mathbf{g}(v)+\mathsf{B}_r(v)\cdot\int dv'(v')^2\,\mathbf{g}(v')=\mathbf{h}(v)\ , \tag{3.11}$$

where the matrix elements of $\mathsf{A}(v)$ and $\mathsf{B}_r(v)$ are

$$\mathsf{A}_{\{\mathbf{k}lm|\mathbf{k}'l'm'\}}(v)=i\omega\delta_{\mathbf{k}\mathbf{k}'}\delta_{ll'}\delta_{mm'}$$
$$+\left[\frac{3(2l'+1)}{4\pi(2l+1)}\right]^{1/2}\langle l'100|l'1l0\rangle\langle l'1m',m-m'|l'1lm\rangle\nu_{m-m'}(\mathbf{k},v)\delta_{\mathbf{k}\mathbf{k}'}+\gamma(\mathbf{k}-\mathbf{k}')\delta_{ll'}\delta_{mm'}\ , \tag{3.12}$$

$$\mathsf{B}_{r\{\mathbf{k}lm|\mathbf{k}'l'm'\}}(v)=-\frac{1}{v_F^2}\delta(v_F-v)\gamma(\mathbf{k}-\mathbf{k}')\delta_{ll'}\delta_{mm'}\delta_{l0}\delta_{m0}\ , \tag{3.13}$$

and the vector $\mathbf{h}(v)$ is

$$h_{\{\mathbf{k}lm\}}=-\left[\frac{4\pi}{3}\right]^{1/2}\frac{en_0}{m}\frac{1}{V_F}\delta(v_F-v)\delta_{l0}\delta_{m0}\ . \tag{3.14}$$

The three components of $\mathbf{k}$ label components of $\mathbf{g}(v)$ as well as the indices l and m. Equation (3.10) can be inverted using the matrix analogues of standard techniques for solving integral equations with a separable kernel. Define the vector $\mathbf{N}$ as

$$\mathbf{N}=\int dv'(v')^2\,\mathbf{g}(v')\ . \tag{3.15}$$

Using (3.15) in (3.11) we can easily solve for $\mathbf{g}(v)$,

$$\mathbf{g}(v)=\mathsf{A}^{-1}(v)\cdot\mathbf{h}(v)-\mathsf{A}^{-1}(v)\cdot\mathsf{B}_r(v)\cdot\mathbf{N}\ . \tag{3.16}$$

Multiplying (3.16) by v^2 and integrating over v we get the closed equation

$$\mathbf{N}=\int dv\, v^2\mathsf{A}^{-1}(v)\cdot\mathbf{h}(v)-\int dv\, v^2\mathsf{A}^{-1}(v)\cdot\mathsf{B}_r(v)\cdot\mathbf{N}$$

which can be solved for $\mathbf{N}$ to get

$$\mathbf{N}=\left[1+\int dv\, v^2\mathsf{A}^{-1}(v)\cdot\mathsf{B}_r(v)\right]^{-1}\int dv\, v^2\mathsf{A}^{-1}(v)\cdot\mathbf{h}(v)\ . \tag{3.17}$$

Equations (3.16) and (3.17) constitute a complete solution to Eq. (3.11).

A problem arises with (3.17). If we try to solve the ordinary Drude model with this formalism we find that the matrix

$$\left[1+\int dv\, v^2\mathsf{A}^{-1}(v)\cdot\mathsf{B}_r(v)\right] \tag{3.18}$$

is not invertible on the one-dimensional subspace spanned by the vector $g_{l=0,\,m=0}(\mathbf{k}=\mathbf{0},\,v)$ at zero frequency. Although we have not been able to show this analytically, numerical results indicate that this continues to be true in the case of inhomogeneous scattering. However, the one-particle distribution function must satisfy the normalization condition

$$n_0=\int\frac{d^3r}{L^3}\int d^3v\, f\ .$$

From (2.11) and (2.12) we see that the full normalization is carried by f_0. Therefore, the $l=0$, $m=0$, $\mathbf{k}=\mathbf{0}$ component of the vector $\mathbf{N}$ must vanish and we can drop this term from Eq. (3.17). The matrix (3.18) appears to be invertible on the remaining vector space at all frequencies. The vector $\mathbf{N}$ is constructed by using (3.17) on the subspace orthogonal to $g_{00}(0,v)$ and setting the component labeled by $l=0$, $m=0$, $\mathbf{k}=\mathbf{0}$ equal to zero.

The formalism we have developed so far is completely general but it is not practical for an arbitrary choice of $\gamma(\mathbf{r})$. If we have to consider all the $\mathbf{k}$'s within even a small sphere in $\mathbf{k}$ space (assuming that we truncate our expansion by requiring $k<k_{\max}$ for some appropriate value of $k_{\max}$) we quickly end up with an enormous number of basis vectors. To avoid this problem, we consider $\gamma(\mathbf{r})$ of the form

$$\gamma(\mathbf{r})=\nu_0+\gamma'(x)+\gamma'(y)+\gamma'(z)\ . \tag{3.19}$$

For the cubic systems considered in this paper, the form (3.19) implies that the scattering is higher at the edges and corners of intersecting grain boundaries than at the center of grain-boundary faces. However, this is not a serious drawback since we expect that the same is true in real systems. The Fourier components of $\gamma(\mathbf{r})$ are

$$\gamma(\mathbf{k})=\nu_0\delta_{\mathbf{k}0}+\gamma'(k_x)\delta_{k_y0}\delta_{k_z0}+\gamma'(k_y)\delta_{k_x0}\delta_{k_z0}+\gamma'(k_z)\delta_{k_x0}\delta_{k_y0}\ . \tag{3.20}$$

The only nonzero components of $\gamma(\mathbf{k})$ are along the $\mathbf{k}$-space axes, which has some interesting consequences. From the explicit expressions for $\mathsf{A}(v)$ and $\mathsf{B}_r(v)$ given by (3.12) and (3.13), we see that there are *no* matrix elements that couple a component of $\mathbf{g}(v)$ that is on the $\mathbf{k}$-space axes with an off-axes component. Thus, if $\gamma(\mathbf{k})$ is of the form (3.20), then the only nonzero components of $\mathbf{g}(v)$ are also on the $\mathbf{k}$-space axes. The volume of $\mathbf{k}$ space that we have to deal with is then effectively one dimensional. This is a considerable reduction in the basis set. The fact that the $g_{lm}(\mathbf{k},v)$ vanish if $\mathbf{k}$ does not lie on the $\mathbf{k}$-space axes implies that in coordinate space g is of the form

$$g=g_0(\mathbf{v})+g_x(x,\mathbf{v})+g_y(y,\mathbf{v})+g_z(z,\mathbf{v})\ . \tag{3.21}$$

This form simplifies the inclusion of the local-field term in the next section.

IV. INCLUSION OF THE LOCAL FIELDS

To derive the matrix elements for the local-field term we assume that (3.21) continues to hold true when the local-field terms are added back in. After we complete the calculation we can verify this assumption *a posteriori*. $g_0(\mathbf{v})$ in (3.21) can be fixed by requiring that $g_x(x,\mathbf{v})$, $g_y(y,\mathbf{v})$, and $g_z(z,\mathbf{v})$ vanish when averaged over all space. The spatially varying part of g is then completely isolated in the $g_x(x,\mathbf{v})$, etc. Substituting (3.21) into the local-field term in (2.15) gives

$$\begin{aligned}\mathcal{J}_{\mathrm{LF}}&\equiv\frac{e^2}{\epsilon_0 m}\left[\int d^3r'\frac{\mathbf{r}-\mathbf{r}'}{|\mathbf{r}-\mathbf{r}'|^3}\int d^3v'\, g\right]\cdot\nabla_{\mathbf{v}}f_0\\&=\frac{e^2}{\epsilon_0 m}\left[\int d^3r'\frac{\mathbf{r}-\mathbf{r}'}{|\mathbf{r}-\mathbf{r}'|^3}\int d^3v'\, g_x(x',\mathbf{v}')\right.\\&\quad+\int d^3r'\frac{\mathbf{r}-\mathbf{r}'}{|\mathbf{r}-\mathbf{r}'|^3}\int d^3v'\, g_y(y',\mathbf{v}')\\&\quad\left.+\int d^3r'\frac{\mathbf{r}-\mathbf{r}'}{|\mathbf{r}-\mathbf{r}'|^3}\int d^3v'\, g_z(z',\mathbf{v}')\right]\cdot\nabla_{\mathbf{v}}f_0\ .\end{aligned} \tag{4.1}$$

The charge fluctuations appearing in each of the integrals in (4.1) are one dimensional. We can do the remaining two spatial integrations analytically to get

$$\mathcal{J}_{\rm LF}=\frac{2\pi e^2}{\epsilon_0 m}\left[\hat{\mathbf{x}}\int_{-\infty}^{\infty}dx'[2\Theta(x-x')-1]\int d^3v'\,g_x(x',\mathbf{v}')+\hat{\mathbf{y}}\int_{-\infty}^{\infty}dy'[2\Theta(y-y')-1]\int d^3v'\,g_y(y',\mathbf{v}')\right.$$
$$\left.+\hat{\mathbf{z}}\int_{-\infty}^{\infty}dz'[2\Theta(z-z')-1]\int d^3v'\,g_z(z',\mathbf{v}')\right]\cdot\nabla_{\mathbf{v}}f_0\ . \tag{4.2}$$

$\hat{\mathbf{x}}$, $\hat{\mathbf{y}}$, and $\hat{\mathbf{z}}$ are unit vectors pointing along the coordinate axes. Equation (4.2) follows immediately from the fact that the electric field propagator for a sheet of charge located at x' and parallel to the (y,z) plane is

$$2\pi[2\Theta(x-x')-1]\ .$$

(Recall that the electric field due to a uniform sheet of charge is constant on either side of the sheet.)

The $g_i(x_i,\mathbf{v})$, where $i=x,y,z$, have the expansions

$$g_i(x_i,\mathbf{v})=\sum_{k_i}\sum_{l,m}(1-\delta_{k_i0})g_i(k_i,v)e^{ik_ix_i}Y_{lm}(\theta,\phi)\ . \tag{4.3}$$

We can leave out the $k_i=0$ term since the $k_i=0$ dependence has been absorbed in $g_0(\mathbf{v})$. Using (4.3) in (4.2) gives

$$\mathcal{J}_{\rm LF}=-\frac{2\pi e^2 n_0}{\epsilon_0 m}\sqrt{4\pi}\frac{1}{V_F}\delta(v_F-v)\left[\sum_{k_x}(1-\delta_{k_x0})\frac{v_x}{v}\int_{-\infty}^{\infty}dx'[2\Theta(x-x')-1]\int d^3v'\,g_{x00}(k_x,v')e^{ik_xx'}\right.$$
$$+\sum_{k_y}(1-\delta_{k_y0})\frac{v_y}{v}\int_{-\infty}^{\infty}dy'[2\Theta(y-y')-1]\int d^3v'\,g_{y00}(k_y,v')e^{ik_yy'}$$
$$\left.+\sum_{k_z}(1-\delta_{k_z0})\frac{v_z}{v}\int_{-\infty}^{\infty}dz'[2\Theta(z-z')-1]\int d^3v'\,g_{z00}(k_z,v')e^{ik_zz'}\right]\ . \tag{4.4}$$

The problem of evaluating the spatial integrals in (4.4) is greatly complicated by the long-range nature of the Coulomb potential. It can be seen by inspection that the integrals

$$\int_{-\infty}^{\infty}dx'[2\Theta(x-x')-1]e^{ik_xx'} \tag{4.5}$$

are not well defined since the integrands do not vanish as $|x|\to\infty$. To make the integrals convergent, we introduce a screened form of the propagator and then take the limit that the screening goes to zero. We replace the step-function propagator in (4.4) by

$$[2\Theta(x-x')-1]e^{-|x-x'|\eta}\ ,$$

where η is an arbitrarily small positive constant. The integrals we must now evaluate are

$$\int_{-\infty}^{\infty}dx'[2\Theta(x-x')-1]e^{-|x-x'|\eta+ik_xx'}$$
$$=\left[\frac{1}{ik_x+\eta}+\frac{1}{ik_x-\eta}\right]e^{ik_xx}\ . \tag{4.6}$$

We can safely let $\eta\to 0$ since the two δ functions that are produced cancel. There is no problem with small $\mathbf{k}$ since we never have to consider $k_x=0$ in Eq. (4.4). Using Eq. (4.6) in (4.4) we can write

$$\mathcal{J}_{\rm LF}=-\frac{2\pi e^2 n_0}{\epsilon_0 m}\sqrt{4\pi}\frac{1}{V_F}\delta(v_F-v)\left[\sum_{k_x}\sum_{k_x'}\left[\frac{2}{ik_x}(1-\delta_{k_x0})\delta_{k_xk_x'}\right]\frac{v_x}{v}\int dv'\,(v')^2g_{x00}(k_x',v')e^{ik_xx}\right.$$
$$+\sum_{k_y}\sum_{k_y'}\left[\frac{2}{ik_y}(1-\delta_{k_y0})\delta_{k_yk_y'}\right]\frac{v_y}{v}\int dv'\,(v')^2g_{y00}(k_y',v')e^{ik_yy}$$
$$\left.+\sum_{k_z}\sum_{k_z'}\left[\frac{2}{ik_z}(1-\delta_{k_z0})\delta_{k_zk_z'}\right]\frac{v_z}{v}\int dv'\,(v')^2g_{z00}(k_z',v')e^{ik_zz}\right]\ . \tag{4.7}$$

The only remaining step is to replace the v_i/v in (4.7) by their spherical harmonics expansions. $\mathcal{J}_{\rm LF}$ becomes

$$\mathcal{J}_{\mathrm{LF}}=-\frac{2\pi e^2 n_0}{\epsilon_0 m}\sqrt{4\pi}\frac{1}{V_F}\delta(v_F-v)$$
$$\times\sum_{l,m}\sum_{l',m'}\left\{\sum_{k_x}\sum_{k_x'}\left[\frac{2}{ik_x}(1-\delta_{k_x0})\delta_{k_xk_x'}\right]\left[\left[\frac{2\pi}{3}\right]^{1/2}(-\delta_{l1}\delta_{m1}+\delta_{l1}\delta_{m,-1})\right]\delta_{l'0}\delta_{m'0}\int dv'\,(v')^2 g_{xl'm'}(k_x',v')e^{ik_x x}\right.$$
$$+\sum_{k_y}\sum_{k_y'}\left[\frac{2}{ik_y}(1-\delta_{k_y0})\delta_{k_yk_y'}\right]\left[i\left[\frac{2\pi}{3}\right]^{1/2}(\delta_{l1}\delta_{m1}+\delta_{l1}\delta_{m,-1})\right]\delta_{l'0}\delta_{m'0}\int dv'\,(v')^2 g_{yl'm'}(k_y',v')e^{ik_y y}$$
$$\left.+\sum_{k_z}\sum_{k_z'}\left[\frac{2}{ik_z}(1-\delta_{k_z0})\delta_{k_zk_z'}\right]\left[\frac{4\pi}{3}\right]^{1/2}\delta_{l1}\delta_{m0}\delta_{l'0}\delta_{m'0}\int dv'\,(v')^2 g_{zl'm'}(k_z',v')e^{ik_z z}\right\}Y_{lm}(\theta,\phi)\ . \tag{4.8}$$

From (4.8) it is clear that the local fields contribute a term

$$\mathsf{B}_s(v)\cdot\int dv'\,(v')^2\mathbf{g}(v')$$

to the left-hand side of (3.11). The matrix elements of $\mathsf{B}_s(v)$ are

$$\mathsf{B}_{s\{k_x lm|k_x'l'm'\}}(v)=-\frac{2\pi e^2 n_0}{\epsilon_0 m}\sqrt{4\pi}\frac{1}{V_F}\delta(v_F-v)\left[\frac{2}{ik_x}(1-\delta_{k_x0})\delta_{k_xk_x'}\right]\left[\frac{2\pi}{3}\right]^{1/2}(-\delta_{l1}\delta_{m1}+\delta_{l1}\delta_{m,-1})\delta_{l'0}\delta_{m'0}\ ,$$
$$\mathsf{B}_{s\{k_y lm|k_y'l'm'\}}(v)=-\frac{2\pi e^2 n_0}{\epsilon_0 m}\sqrt{4\pi}\frac{1}{V_F}\delta(v_F-v)\left[\frac{2}{ik_y}(1-\delta_{k_y0})\delta_{k_yk_y'}\right]i\left[\frac{2\pi}{3}\right]^{1/2}(\delta_{l1}\delta_{m1}+\delta_{l1}\delta_{m,-1})\delta_{l'0}\delta_{m'0}\ , \tag{4.9}$$
$$\mathsf{B}_{s\{k_z lm|k_z'l'm'\}}(v)=-\frac{2\pi e^2 n_0}{\epsilon_0 m}\sqrt{4\pi}\frac{1}{V_F}\delta(v_F-v)\left[\frac{2}{ik_z}(1-\delta_{k_z0})\delta_{k_zk_z'}\right]\left[\frac{4\pi}{3}\right]^{1/2}\delta_{l1}\delta_{m0}\delta_{l'0}\delta_{m'0}\ .$$

Since none of the matrix elements of $\mathsf{B}_s(v)$ connect a component of $\mathbf{g}(v)$ that is on the $\mathbf{k}$-space axes with an off-axis component, the assumption that g remains in the form (3.21) when the local fields are included is verified.

V. CUBIC CRYSTALLITES

So far we have not specified the form of $\gamma'(x)$ appearing in (3.19). For the calculations in this paper we choose

$$\gamma'(x)=\sum_{n=-\infty}^{\infty}\nu'\frac{2}{\sqrt{\pi}}e^{-4(x-nL)^2/w^2}\ . \tag{5.1}$$

This is a Gaussian-shaped grain boundary with full width w and height $2\nu'/\sqrt{\pi}$. The Fourier coefficients are also Gaussians,

$$\gamma'(k_x)=\nu'\frac{w}{L}e^{-k_x^2w^2/16}\ . \tag{5.2}$$

If we set the intragrain scattering frequency equal to ν_0 then the $\mathbf{k}=\mathbf{0}$ component of $\gamma(\mathbf{k})$ is

$$\gamma_0=\gamma(\mathbf{k}=\mathbf{0})$$
$$=\nu_0+3\nu'\frac{w}{L}\ . \tag{5.3}$$

Equation (5.2) is especially convenient for calculations since it has a rapid falloff for large $|\mathbf{k}|$. As we mentioned earlier, the choice (5.1) for $\gamma'(x)$ leads to grains with higher scattering at the corners and edges of crystallites compared to the center of a crystallite face.

In addition to the choice (3.19) for the $\gamma(\mathbf{r})$, we can use the cubic symmetry of the system to reduce the basis set even further. Although the electric field destroys the symmetry in the z direction, the system remains invariant under $\pi/2$ rotations and inversions in the (x,y) plane. The spherical harmonics transform as follows under inversions with respect to x and y:

$$Y_{lm}(\theta,\pi-\phi)=Y_{l,-m}(\theta,\phi)\quad(x\to-x)\ ,$$
$$Y_{lm}(\theta,-\phi)=(-1)^m Y_{l,-m}(\theta,\phi)\quad(y\to-y)\ .$$

If we rotate the system by $\pi/2$ in the (x,y) plane, then the spherical harmonics transform as

$$Y_{lm}(\theta,\phi+\pi/2)=(i)^m Y_{lm}(\theta,\phi)\ .$$

This leads to the following relations between the $g_{lm}(\mathbf{k},v)$:

$$g_{lm}(k_x,k_y,k_z,v)=g_{l,-m}(-k_x,k_y,k_z,v)$$
$$=(-1)^m g_{l,-m}(k_x,-k_y,k_z,v)$$
$$=(i)^m g_{lm}(k_y,-k_x,k_z,v)\ . \tag{5.4}$$

Because of these relations we only need to calculate the $g_{lm}(\mathbf{k},v)$ for $\mathbf{k}$'s on the positive k_x axis as well as the k_z axis. We can further show from Eqs. (5.4) that the

$g_{lm}(\mathbf{k},v)$ must vanish if m is odd.

Although the derivations have been performed for a three-dimensional system, it is straightforward to adapt the calculations to a system in which the only spatial inhomogeneities are along the z axis. (To avoid confusion later on, we would like to make it clear that by one dimension we mean a layered system that is only nonuniform in one direction. We are not referring to a wire.) If we use (5.1) to model the spatial dependence of the scattering, then the only other modification we need to make is in the $\mathbf{k}=\mathbf{0}$ component of the scattering frequency,

$$\gamma_0=\nu_0+\nu'\frac{w}{L} .$$

Once g is known, the frequency-dependent conductivity can be evaluated by finding the portion of the electric current that is linear in the external field. This is just

$$\mathbf{j}_e=-e\int d^3v\int\frac{d^3r}{L^3}\mathbf{v}g\mathbf{E}_{\text{ext}} .$$

The conductivity is a tensor quantity, but for a system with cubic symmetry it is proportional to the unit tensor and we can define the scalar conductivity as being equal to the zz component. The scalar conductivity is then

$$\sigma(w)=-e\int d^3v\int\frac{d^3r}{L^3}v_z g$$
$$=-e\int v^3dv\left[\frac{4\pi}{3}\right]^{1/2}g_{10}(\mathbf{k}=0,v) . \quad (5.5)$$

In order to distinguish easily Drude-like behavior from non-Drude behavior it is convenient to rewrite the conductivity in terms of a frequency-dependent scattering rate. For constant γ the Drude conductivity is

$$\sigma_D(\omega)=\frac{n_0e^2}{m}\frac{1}{\gamma+i\omega} .$$

However, *any* conductivity can be written as

$$\sigma(\omega)=\frac{n_0e^2}{m}\frac{1}{\gamma(\omega)+i\omega} .$$

Solving for $\gamma(\omega)$ we have

$$\gamma(\omega)=\frac{n_0e^2}{m}\frac{1}{\sigma(\omega)}-i\omega . \quad (5.6)$$

The advantage of writing the conductivity in this form is that we can immediately spot non-Drude behavior. Drude-like behavior leads to a real $\gamma(\omega)$ with no frequency dependence, while a complex, frequency-dependent $\gamma(\omega)$ points to a non-Drude system.

Since the frequency-dependent conductivity is not, in general, directly accessible from experiment we also calculate the reflectance spectra. We briefly sketch the relationship between conductivity and reflectance.[20] The frequency-dependent dielectric function can be calculated from the conductivity via

$$\epsilon(\omega)=\epsilon_0+4\pi i\frac{\sigma(\omega)}{\omega} .$$

If we define ϵ_1 and ϵ_2 as the real and imaginary parts of $\epsilon(\omega)$, respectively, then the extinction coefficient α and the refractive index η are

$$\alpha^2=\frac{-\epsilon_1+(\epsilon_1^2+\epsilon_2^2)^{1/2}}{2} ,$$
$$\eta^2=\frac{\epsilon_1+(\epsilon_1^2+\epsilon_2^2)^{1/2}}{2} .$$

From these the reflectance R is

$$R=\frac{(\eta-1)^2+\alpha^2}{(\eta+1)^2+\alpha^2} .$$

To actually do calculations we had to choose truncation criteria for both the $\mathbf{k}$'s and the spherical harmonics. The only values of $\mathbf{k}$ that we have to consider are along the axes and these are a unit vector multiplied by $\pm 2\pi n/L$ for some integer n. Truncating the $\mathbf{k}$'s is equivalent to picking a value of $n_{\max}$ such that $n\le n_{\max}$. We found that using

$$n_{\max}=\frac{L}{w}$$

gave very good results. Similarly, we truncated the spherical harmonics by requiring that $l\le l_{\max}$. We used the value $l_{\max}=1$ in our calculations. We checked these truncations by independently doubling $n_{\max}$ from 10 to 20 and increasing $l_{\max}$ from 1 to 2 for the results shown in Figs. 1 and 2. The maximum change in the frequency-dependent scattering, $\gamma(\omega)$, was less than 3% and the change in the reflectance spectrum was undetectable.

For the calculations in this paper we use parameters appropriate to heavily doped tin oxide.[4] We chose $n_0=4.2\times10^{21}$ e/cm^3, $\epsilon_0=4.0$, $m=0.281m_e$, and $\nu_0=2.0\times10^{14}$ s^{-1}. The parameters describing the grain boundaries themselves are more problematical. We set the crystallite size to $L=1000$ Å and investigated a number of different widths and heights. We tried grain-boundary widths of 50 and 100 Å. These values may appear to be too broad, but there are a number of reasons for using wide grain boundaries, beside the obvious one that the calculations are easier to do when L/w is small. One is that the grain boundaries may be physically wide. In pure systems the grain boundary probably extends over a couple of atomic spacings, but in heavily doped systems it is possible that the dopant segregates preferentially in the grain boundaries, resulting in an anomalously high concentration of impurity in the intergrain region. These impurities could then back diffuse into the crystal grains slightly so that the region of higher scattering extends beyond the actual grain boundary.

A second reason involves the distribution of sizes in actual polycrystalline samples. Most samples do not consist of a regular array of crystallites; instead there is a distribution of sizes and shapes. In come cases, the variation is large enough so that the sample can be considered to be composed of large crystallies with smaller crystallites filling in the interstitial regions. These smaller crystallites can be thought of as an effective grain boundary

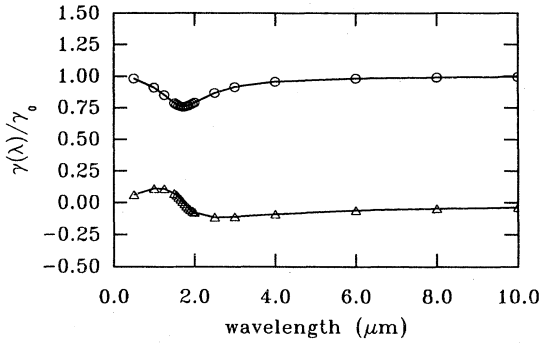

FIG. 1. The real and imaginary parts of $\gamma(\lambda)$ for a one-dimensional layered system. The grain-boundary scattering amplitude is $\nu'/\nu_0=5.0$ and the grain-boundary width is $w=100$ Å. The open circles (○) are Re$[\gamma(\lambda)/\gamma_0]$ and the open triangles (△) are Im$[\gamma(\lambda)/\gamma_0]$.

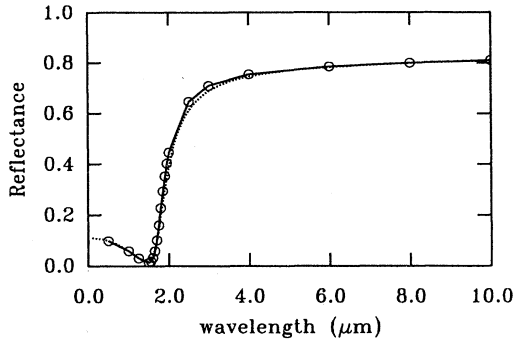

FIG. 3. The reflectance spectrum for a one-dimensional layered system. The grain-boundary scattering amplitude is $\nu'/\nu_0=5.0$ and the grain-boundary width is $w=50$ Å. The dotted curve is an ordinary Drude spectrum calculated for a value of $\gamma=2.55\times10^{14}\ \mathrm{s}^{-1}$.

with a broad width. Even in fairly uniform samples the fluctuations in crystallite sizes should lead to an effective width that is larger than the physical width of a single grain boundary.

We begin by considering a system that is nonuniform only along the z axis. The grain boundaries are planes at distances L apart and parallel to the $z=0$ plane. The grain-boundary width is set at $w=100$ Å and we choose the amplitude of scattering in the grain boundary so that $\nu'/\nu_0=5.0$. In Fig. 1 we plot the real and imaginary parts of $\gamma(\lambda)$ as a function of the wavelength of light. It is immediately evident that $\gamma(\lambda)$ exhibits non-Drude behavior. Not only is $\gamma(\lambda)$ complex but there is a complicated dependence of $\gamma(\lambda)$ on wavelength. At short wavelength (high frequency) the real part of $\gamma(\lambda)/\gamma_0$ goes to 1 and the imaginary part vanishes. At high frequency, the electrons do not have much time to move in the external field before they are forced to change direction. They oscillate in tight orbits that only sample the local environment. The conductivity is then the average of the conductivities over all the local environments and can be written as

$$\sigma(\omega)\simeq\frac{n_0e^2}{m}\int\frac{dz}{L}\frac{1}{\gamma(z)+i\omega}$$
$$\simeq\frac{n_0e^2}{m}\left[\frac{1}{i\omega}+\frac{1}{\omega^2}\int\frac{dz}{L}\gamma(z)\right]$$
$$\simeq\frac{n_0e^2}{m}\frac{1}{\gamma_0+i\omega}\ .$$

This can also be verified analytically by observing that the matrix $\mathsf{A}(v)$ is diagonal and proportional to ω at high frequencies. As the frequency drops the trajectories spread out, the electrons sample several different environments, and $\gamma(\lambda)$ deviates from γ_0. There appears to be some kind of resonance in $\gamma(\lambda)$ in the neighborhood of the plasma wavelength at $\lambda_{\mathrm{pl}}=1.72$ μm. (The plasma wavelength can be calculated from the plasma frequency, which is given by $\Omega_{\mathrm{pl}}^2=4\pi n_0e^2/\epsilon_0m$.) At long wavelengths, the real part of the scattering rate goes all the way back up to the value γ_0 while the imaginary part has a negative tail that is decaying to zero.

In Fig. 2 we plot the corresponding reflectance spectrum, along with a Drude curve whose scattering fre-

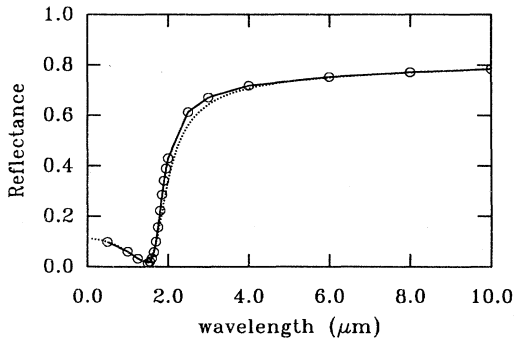

FIG. 2. The reflectance spectrum for a one-dimensional layered system. The grain-boundary scattering amplitude is $\nu'/\nu_0=5.0$ and the grain-boundary width is $w=100$ Å. The dotted curve is an ordinary Drude spectrum calculated for a value of $\gamma=3.05\times10^{14}\ \mathrm{s}^{-1}$.

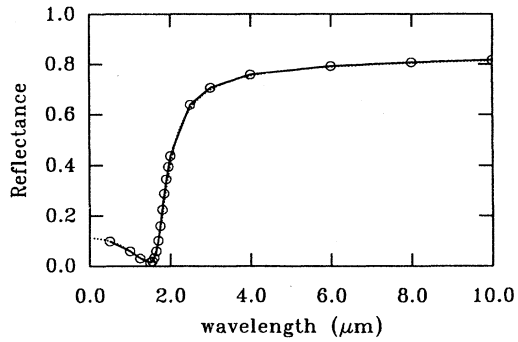

FIG. 4. The reflectance spectrum for a one-dimensional layered system. The grain-boundary scattering amplitude is $\nu'/\nu_0=2.0$ and the grain-boundary width is $w=100$ Å. The dotted curve is an ordinary Drude spectrum calculated for a value of $\gamma=2.45\times10^{14}\ \mathrm{s}^{-1}$.

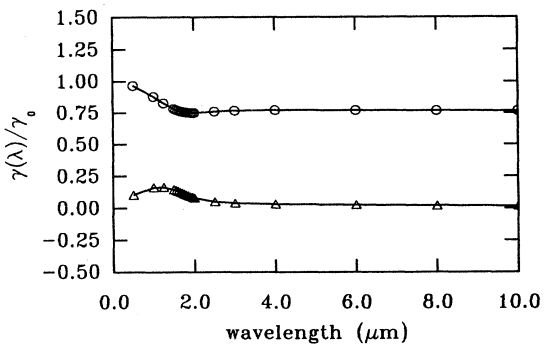

FIG. 5. The real and imaginary parts of $\gamma(\lambda)$ for a three-dimensional cubic system. The grain-boundary scattering amplitude is $\nu'/\nu_0=5.0$ and the grain-boundary width is $w=100$ Å. The open circles ($\circ$) are $\mathrm{Re}[\gamma(\lambda)/\gamma_0]$ and the open triangles ($\triangle$) are $\mathrm{Im}[\gamma(\lambda)/\gamma_0]$.

quency has been adjusted so that it matches the grain-boundary curve at $\lambda=10$ μm. The Drude curve actually undercuts the grain-boundary curve in the vicinity of the shoulder at 2 μm. This is the opposite of most deviations that are seen experimentally.

To investigate the effect of grain-boundary width on the results we reduced w to $w=50$ Å. The qualitative behavior of $\gamma(\lambda)$ is approximately the same as that shown in Fig. 1. The reflectance spectrum is shown in Fig. 3. For these parameters the grain-boundary curve and the low-frequency Drude fit are very close, although the Drude curve still undercuts the grain-boundary curve near 2 μm.

To complete our investigation of one-dimensional layered systems, we try lowering ν'/ν_0 to $\nu'/\nu_0=2.0$ and use a grain-boundary width of $w=100$ Å. The reflectance spectrum is plotted in Fig. 4. In this case it is almost indistinguishable from a Drude curve. These results suggest that the scattering amplitude in the grain boundary is slightly more important than the width in producing non-Drude behavior in the reflectance spectrum.

In three dimensions the behavior of $\gamma(\lambda)$ changes qualitatively. In Fig. 5 we plot $\gamma(\lambda)$ for a grain-boundary width of $w=100$ Å and a scattering amplitude of $\nu'/\nu_0=5.0$. At long wavelengths, the real part of $\gamma(\lambda)$ drops to a value that is noticeably lower than the average value γ_0. In one-dimensional layered systems, the real part of $\gamma(\lambda)$ returned to γ_0 at long wavelengths. If we ignore the local fields, the one-dimensional system can be considered as a set of resistors in series. The scattering frequencies for each resistor, which are proportional to the resistances, can all be added together and the average resistance is then given by γ_0. This accounts for the return of $\mathrm{Re}[\gamma(\lambda)]$ to γ_0 at long wavelengths in one dimension. In three dimensions, this picture breaks down since there should be less current flow in the grain boundaries parallel to the external field than in the intragrain region and this results in the lower scattering at large λ. There is still a tail in $\mathrm{Im}[\gamma(\lambda)]$ at long wavelengths but this is now positive instead of negative.

The corresponding reflectance spectrum is plotted in Fig. 6. This is almost indistinguishable from a Drude spectrum, although the grain-boundary curve does slightly undercut the low-frequency Drude fit near 2 μm. This is often seen experimentally, although the deviations from a Drude curve are often larger.[1-4] Interestingly, if we decrease the scattering amplitude to $\nu'/\nu_0=2.0$ the deviations from the long-wavelength Drude-fit increase, as can be seen in Fig. 7.

To summarize, in one dimension the deviations from a Drude curve are the opposite of those seen experimentally, while in three dimensions the deviations are the same. However, the deviations shown in Figs. 6 and 7 represent a maximum and we have been unable to find experimentally plausible parameters that increase the deviation. Nevertheless, actual polycrystalline samples often differ from a Drude curve by substantially larger amounts. One possible source of these larger differences is the disorder that exists in real polycrystalline samples. Unfortunately, numerical limitations have prevented us from exploring this idea fully, but we have some preliminary results in one dimension that indicate that variations in the crystallite sizes can further influence the conductivity.

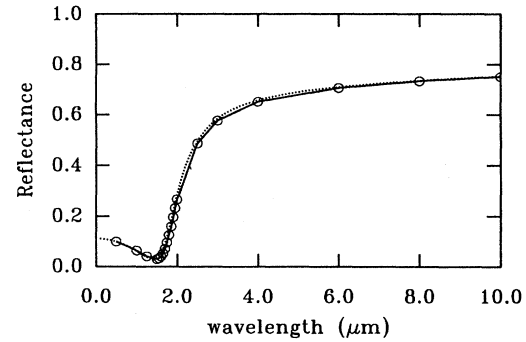

FIG. 6. The reflectance spectrum for a three-dimensional cubic system. The grain-boundary scattering amplitude is $\nu'/\nu_0=5.0$ and the grain-boundary width is $w=100$ Å. The dotted curve is an ordinary Drude spectrum calculated for a value of $\gamma=3.75\times10^{14}$ s^{-1}.

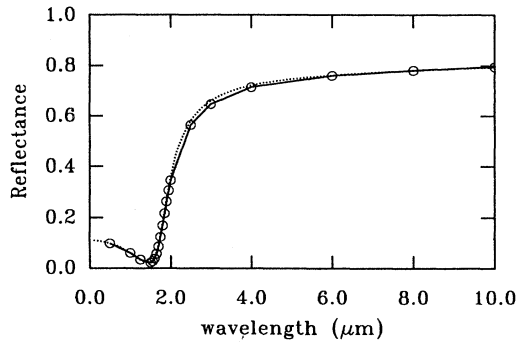

FIG. 7. The reflectance spectrum for a three-dimensional cubic system. The grain-boundary scattering amplitude is $\nu'/\nu_0=2.0$ and the grain-boundary width is $w=100$ Å. The dotted curve is an ordinary Drude spectrum calculated for a value of $\gamma=2.85\times10^{14}$ s^{-1}.

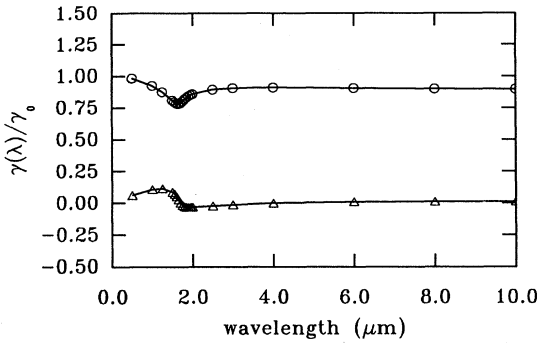

FIG. 8. The real and imaginary parts of $\gamma(\lambda)$ for a layered system with three crystallite sizes. The total size of the unit cell is 3000 Å and the grain boundaries are located at 0, 800, and 2000 Å. The grain-boundary scattering amplitude is $\nu'/\nu_0=5.0$ and the grain-boundary width is $w=100$ Å. The open circles (○) are $\mathrm{Re}[\gamma(\lambda)/\gamma_0]$ and the open triangles (△) are $\mathrm{Im}[\gamma(\lambda)/\gamma_0]$.

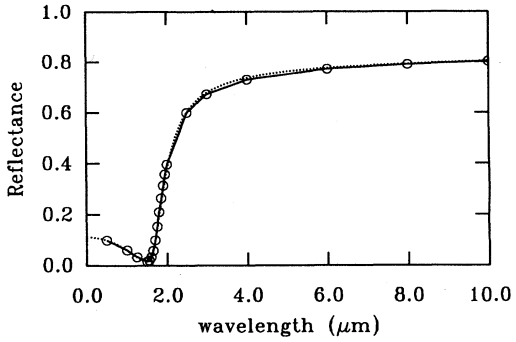

FIG. 9. The reflectance spectrum for a layered system with three crystallite sizes. The total size of the unit cell is 3000 Å and the grain boundaries are located at 0, 800, and 2000 Å. The grain-boundary scattering amplitude is $\nu'/\nu_0=5.0$ and the grain-boundary width is $w=100$ Å. The dotted curve is an ordinary Drude spectrum calculated for a value of $\gamma=2.65\times10^{14}$ s^{-1}.

Instead of a simply periodic one-dimensional system composed of a single 1000-Å crystallite we increase the unit cell size to 3000 Å and locate grain boundaries at 0, 800, and 2000 Å. The average size of the crystallites is still 1000 Å, but there is some variation about the mean. We again set $w=100$ Å and use a scattering amplitude of $\nu'/\nu_0=5.0$. In Fig. 8 we plot $\gamma(\lambda)$ as a function of λ. This should be compared to Fig. 1. The two most significant changes are that $\mathrm{Re}[\gamma(\lambda)]$ is still below γ_0 at 10 μm, while in Fig. 1 it has risen to γ_0 by about 4 μm. Furthermore, the tail at long wavelengths in $\mathrm{Im}[\gamma(\lambda)]$ is much smaller than in Fig. 1 and has even changed sign. There are clearly interference effects between the different size crystallites that act to decrease the low-frequency scattering. The reflectance spectrum is shown in Fig. 9 and should be compared to the spectrum shown in Fig. 2. The grain-boundary spectrum now undercuts the Drude curve near the shoulder at 2 μm, whereas in Fig. 1 it overshot the Drude curve in this region. Clearly, disorder can further alter the results although at present we cannot say by how much.

ACKNOWLEDGMENTS

We are indebted to Dr. Jim Proscia for many useful discussions and to Professor David Vanderbilt for suggesting the use of a screened propagator and Professor Bert Halperin for suggesting the local-equilibrium form of the collision operator. We thank the National Science Foundation, the Solar Energy Research Institute (Golden, CO) and the Harvard University Materials Research Laboratory for financial support, and the John von Neumann Computer Center, Consortium for Scientific Computing (Princeton, N.J.), for a grant of computer time.

[1]Von R. Groth, E. Kauer, and P. C. V. D. Linden, Z. Naturforsch. **179**, 789 (1962).
[2]J. C. C. Fan and F. J. Bachner, J. Electrochem. Soc. **122**, 1719 (1975).
[3]F. Simonis, M. van der Leij, and C. J. Hoogendorn, Sol. Energy Mater. **1**, 221 (1979).
[4]J. Proscia, Ph. D. thesis, Harvard University, 1988.
[5]E. H. Sondheimer, Proc. R. Soc. London **203**, 75 (1950).
[6]F. Garcia Moliner and S. Simons, Proc. Cambridge Philos. Soc. **53**, 848 (1957).
[7]D. V. Gitsu, I. M. Golban, and V. G. Kantser, Phys. Status Solidi B **112**, 473 (1982).
[8]P. B. Allen, Phys. Rev. B **13**, 1416 (1976).
[9]P. B. Allen, Phys. Rev. B **17**, 3725 (1978).
[10]F. J. Pinski, Phys. Rev. B **21**, 4380 (1980).
[11]A. F. Mayadas, M. Shatzkes, and J. F. Janak, Appl. Phys. Lett. **14**, 345 (1969).
[12]A. F. Mayadas and M. Shatzkes, Phys. Rev. B **1**, 1382 (1970).
[13]R. A. Brown, J. Phys. F **7**, 311 (1978).
[14]C. R. Tellier, Thin Solid Films **51**, 311 (1978).
[15]C. R. Tellier, A. J. Tosser, and L. Hafid, J. Mater. Sci. **15**, 2875 (1980).
[16]J. M. Ziman, *Principles of the Theory of Solids,* 2nd ed. (Cambridge University Press, Cambridge, 1972).
[17]N. W. Ashcroft and N. D. Mermin, *Solid State Physics* (Saunders College, Philadelphia, 1976).
[18]E. Merzbacher, *Quantum Mechanics,* 2nd ed. (Wiley and Sons, New York, 1951).
[19]E. U. Condon and G. H. Shortley, *The Theory of Atomic Spectra* (Cambridge University Press, Cambridge, 1951).
[20]J. R. Dixon, in *Optical Properties of Solids,* edited by S. Nudelman and S. S. Mitra (Plenum, New York, 1969).